Flywheel Energy Storage as an Alternative for Chemical Batteries in Small LEO Satellites: Feasibility and Attitude Impact

Benjamin Spitaels
iMMC
UCLouvain
Louvain-La-Neuve, Belgium
benjamin.spitaels@uclouvain.be

Bruno Dehez
iMMC
UCLouvain
Louvain-La-Neuve, Belgium
bruno.dehez@uclouvain.be

Marc Bekemans
EPL
UCLouvain
Louvain-La-Neuve, Belgium
marc.bekemans@uclouvain.be

***Abstract*— Given the rapidly increasing number of satellites, mainly driven by the deployment of large constellations, manufacturers are under growing pressure to innovate in order to reduce both costs and environmental impact. In this context, the present work investigates the feasibility of replacing chemical batteries on Low Earth Orbit (LEO) satellites with mechanical storage systems based on flywheels. Flywheel Energy Storage Systems (FESS) can offer a significantly higher depth of discharge (easily up to about 75%) compared to conventional chemical batteries (10-20%), thereby enabling reductions in both mass and volume. Despite these advantages, the angular momentum inherent to flywheel operation will significantly perturb the spacecraft's attitude dynamics, posing a major challenge for attitude control. The objective of this study is to develop an innovative solution that provides the required energy storage while cancelling the net impact on satellite attitude. The concept under investigation relies on a pair of counter-rotating magnetically suspended flywheels. This paper presents an overview of the relevant literature, introduces a preliminary concept, and discusses initial simulation results to illustrate its impact on the attitude dynamics of a small LEO satellite.**

Keywords—LEO satellite, power systems, battery, two counter-rotating flywheels, energy storage, magnetic bearings, attitude.

I. Introduction

Over the past decade, the space sector has shifted from traditional geostationary (GEO) satellites toward large constellations of smaller Low Earth Orbit (LEO) platforms designed for 5 to 7-year missions. As of 2026, more than 10,000 satellites are already deployed within the Starlink constellation, and the total number of LEO satellites is expected to exceed 100,000 by 2030 according to the European Space Agency (ESA). This rapid expansion increases the pressure to develop innovative, cost-effective, and sustainable subsystem solutions.

Energy storage remains a critical limitation. LEO satellites experience orbital periods of about 90 minutes, including eclipse phases of 30 to 40 minutes, leading to tens of thousands of charge/discharge cycles over their lifetime. To ensure durability, battery Depth of Discharge (DoD) is typically limited to 10-20%, resulting in more than 80% of the battery mass being effectively dedicated to lifetime rather than usable energy. This constraint significantly reduces system-level efficiency.

Flywheel Energy Storage Systems (FESS) offer a compelling alternative based on kinetic energy storage. They provide long lifetime with low sensitivity to cycling, high usable DoD (75-90%), competitive cost, and reduced volume and mass. In addition, FESSs enable high power pulses and can be coupled with attitude control, further contributing to mass reduction [1]-[8]. Their integration, however, introduces challenges, including disturbances on spacecraft attitude, intrinsic self-discharge (limited in LEO conditions), containment requirements, and launch constraints [4], [5].

This work initiates a study on a high-speed Flywheel Energy Storage System for LEO satellites, with the objective of eliminating its impact on satellite attitude through active magnetic bearing control, while validating their compatibility with spacecraft power buses.

This paper is organized as follows. Section II reviews the state of the art. Section III presents the FESS and its control. Section IV analyzes its impact on satellite attitude through dynamic modeling and simulation, while investigating system non-idealities. Section V proposes a one-axis torque control strategy to partially mitigate its impact on satellite dynamics. Section VI concludes the paper.

II. State of the Art

Early research on electro-mechanical energy storage can be traced back to the work of Roes in 1961 [9], who described a system composed of two magnetically suspended counter-rotating flywheels capable of storing 500 Wh with a specific energy of 15.4 Wh/kg. In the 1970s, Notti et al. [1], [2] introduced the concept of the "Integrated Power/Attitude Control System (IPACS)" in a feasibility study conducted by Rockwell International Space Division for NASA. The IPACS concept relied on an array of spinning wheels able not only to store energy but also to control spacecraft attitude. The analysis was performed considering seven types of space missions, highlighting its compatibility with long missions or missions involving a high number of charge/discharge cycles.

In 1976, Sindlinger from Teldix presented in [10] a five-degree-of-freedom active magnetic bearing momentum wheel (MBMW), enabling three-axis attitude control with a single device. Sindlinger concluded that this technology could be used in an integrated energy storage and attitude control system utilizing a pair of counter-rotating wheels with Vernier gimbaling capability. Similarly, Poubeau [11] described in 1980 a magnetic suspension system for satellite reaction and momentum wheels, which could also help damp satellite nutation. Like Sindlinger, he noted that two counter-rotating flywheels could serve for energy storage, with misalignment compensated by magnetic suspension. Robinson later summarized the European research on flywheel energy storage for space applications in [12], reporting energy densities of approximately 20 Wh/kg.

This work is funded by the Walloon Region (Belgium) and Thales Alenia Space through the Win4Doc program.

In 1983, Keckler reported in [3] on work from NASA Langley Research Center on the IPACS concept, including both simulations and hardware development. In parallel, Rodriguez et al. from NASA Goddard Space Flight Center assessed a "mechanical capacitor" for spacecraft based on flywheels in [4], [5]. Consistent with earlier studies, they compared the performance of two counter-rotating flywheels with chemical batteries, concluded that at least four wheels are required for attitude control, and provided design recommendations for flywheel energy storage systems. NASA's growing interest in Flywheel Energy Storage Systems (FESS) later extended to the International Space Station (ISS). In this context, Oglevie and Eisenhaure (Rockwell International) [13] presented the results of a study on an IPACS concept for the ISS, demonstrating that the approach was not only feasible but offered several advantages. Their proposed system relies on an array of at least five gimbaled units.

In 1995, under a NASA contract, Santo et al. from Rockwell International conducted a feasibility analysis on the use of FESS for space applications [6], including conceptual design of a flywheel demonstrator and a theoretical development plan. Shortly after, Edwards et al. from Boeing and NASA jointly presented in [14] a plan to conduct a flight test demonstration of a FESS on the ISS with an expected lifetime exceeding 10 years. To cancel unwanted angular momentum effects, the proposed demonstration unit consisted of two counter-rotating, magnetically suspended flywheels operating at rotational speeds up to 60 krpm, with a nominal output power above 4.2 kW and an energy capacity greater than 5 kWh. And in 1998, Beaman and Rao from NASA Goddard Space Flight Center discussed in [15] the potential of using a FESS in combination with batteries to improve the performance of LEO spacecraft. They proposed a reference design for such a system, followed by an implementation plan including magnetic bearings and attitude control capability (IPACS).

Concluding decades of research during the 20th century, Pieronek et al. [7] from One Space Park and Christopher and Beach [8] from NASA Lewis Research Center each presented a review of the FESS concept, summarizing its benefits, challenges, and previous developments. In addition, Groom and Britcher published a report [16] about the NASA Fifth International Symposium on Magnetic Suspension Technology, summarizing conference contributions related to magnetically suspended flywheels for energy storage systems (ESS).

While previous work mainly analyzed concept feasibility and focused on energy storage, Hall developed in 1997 in [17] a dynamic model composed of multiple rigid bodies, each containing one or two rotating flywheels, and studied the resulting impact on spacecraft attitude. The results showed that at least four wheels are necessary for an IPACS. In parallel, Roithmayr from NASA Langley Research Center investigated in [18] and [19] the dynamic influence of a FESS and its potential to assist the Control Moment Gyroscopes (CMGs) in ISS attitude control. Two possible contingency scenarios were analyzed and found negligible in impact. Roithmayr later developed [20], [21], in collaboration with Analytical Mechanics Associates Inc., a model combining flywheels and Control Moment Gyroscopes (CMGs) to support the definition of control laws. A control law for attitude control and energy storage was as a result designed and simulated using an efficient feedback method to compensate for rotor damping effects.

At the beginning of the new millennium, from 2000 to 2005, Kenny, Kascak et al. from NASA published a series of articles [22]-[30] on the analysis, development, and control of FESS composed of counter-rotating flywheels for the ISS. Their comprehensive work addressed DC bus power control, the PMSM motor design, and single-axis attitude control capability, supported by simulations and laboratory demonstrations. Around the same time, Jansen and Dever designed a 60 krpm, 525 Wh, 1 kW magnetically suspended flywheel module, designated the G2 module, for laboratory testing at NASA [31]. Its design requirements were built on previous NASA projects, and the module was subsequently utilized by NASA Glenn Research Center.

At the same time in the 2000s, Truong et al. from NASA Glenn Research Center published work on the electrical behavior of flywheels for space applications, considering various bus voltages and flywheel angular velocities [32].

In parallel, Fausz, Richie, and Tsiotras introduced the concept of Variable Speed Control Moment Gyroscopes (VSCMGs) for IPACS applications [33]-[35]. A VSCMG combines a traditional gimballed CMG with a Reaction Wheel (RW). This concept enables not only energy storage and spacecraft attitude control but also improved singularity avoidance. A theoretical model was developed and numerical simulations of a VSCMG pyramid configuration were performed using a "VSCMG Workbench" implemented in Simulink. Over the same period, Tsiotras et al. developed in [36] an algorithm for simultaneous attitude and energy management of spacecraft equipped with a cluster of more than three wheels, defining two perpendicular spaces: one for energy storage and one for attitude control. In parallel, Guyot et al. introduced the Flywheel Power & Attitude Control System (FPACS) concept and analyzed various configurations combining Energy Wheels (EW) and traditional Reaction Wheels (RW) to simultaneously store energy and track spacecraft attitude. Both GEO and LEO missions were considered in their analysis [37]. And until 2004, under Tsiotras' supervision, Yoon continued work on VSCMGs for IPACS as part of his doctoral thesis, extending the model with two control laws specifically designed to handle uncertainties in system parameters [38], [39]. Following up on Fausz, Richie, and Tsiotras, Costic et al. proposed in [40] two non-linear control strategies for an Integrated Energy Management and Attitude Control (IEMAC) system, enabling simultaneous tracking of spacecraft attitude and a power profile. In 2004, Jia et al. first proposed in [41] an evolution of the VSCMG in which each unit consists of two counter-rotating wheels to avoid singularities, and later introduced in [42] a configuration with more than four wheels to prevent individual wheel saturation.

Varatharajoo and Fasoulas presented in [43] and [44] a similar concept, the Combined Energy and Attitude Control System (CEACS), together with a high-level methodology for the simultaneous control of satellite attitude and stored energy, supported by simulation results. They noted that certain issues, such as misalignment, could be mitigated using magnetic bearings. This methodology was later applied to a small satellite in [45], and rotor stress considerations were addressed in [46]. Their work was further extended by Eshghi [47], [48] and Aslam [49] in the following decades.

In 2006, Park et al., supported by NASA, contributed to research on IPACS by first proposing a dynamic model for flexible shafts and bearings [50], then investigating MIMO control for clusters of four or more wheels [51], and later extending VSCMG concepts by introducing magnetic bearings to isolate flywheel imbalances from the spacecraft [52]. In parallel, under Lappas' supervision, Richie continued work on VSCMGs for space applications as part of his thesis [53]-[56], addressing actuator sizing and proposing a new steering law. Years later, Malik and Asghar proposed in [57] a steering law designed to avoid singularities, and similarly, Yao et al. introduced in 2017 [58] a new VSCMG steering law targeting the same objective.

Over the last ten years, much of the interest in this technology has come from Turkey, notably with Aydin and Aydemir in 2016 [59], who designed and implemented an 11 Wh FESS for space applications, and with Çelikel et al. in 2017 [60], who performed experimental studies on a FESS test setup. In 2019, Saad et al. proposed in [61] an evolution of NASA's work by Kenny and Kascak, presenting a FESS for LEO applications based on two counter-rotating wheels to store energy and perform single-axis attitude control. Finally, Sharma and Santasalo-Aarnio [62] reviewed energy storage technologies for space applications in 2025, discussing flywheels, batteries, fuel cells, and supercapacitors.

Storing energy in momentum wheels for space applications as an alternative to chemical batteries has been a subject of interest for several decades. Early studies primarily focused on describing the concept and evaluating its feasibility, while subsequent work proposed various system designs and investigated the possibility of extending the concept to spacecraft attitude control.

The present work initiates the study of a Flywheel Energy Storage System composed of two counter-rotating magnetically suspended flywheels, aimed at storing energy for Low Earth Orbit (LEO) applications. Although related approaches have been reported in the literature, the novelty lies in integrating active magnetic bearings into the torque control, enabling active compensation of parasitic torques along the three axes without disturbing spacecraft attitude. This approach leads to a standalone energy storage solution that could directly replace chemical batteries onboard satellites.

III. Flywheel Energy Storage System

A. Description

The objective of this paper is to introduce ongoing work aimed not at developing a fully optimized, manufacturable Flywheel Energy Storage System (FESS) for space applications, but rather at conducting an extensive analysis to assess the viability of the concept. This includes not only the compatibility of such an energy storage alternative with the power bus of a LEO satellite, but also the analysis and control of its influence on satellite attitude, while considering additional aspects such as ecological impact, internal dissipation, and thermal management.

The currently envisioned FESS concept consists of two counter-rotating, magnetically suspended flywheels, providing four degrees of freedom, in line with typical configurations found in previous studies. These degrees of freedom allow both energy storage and control of the resulting torques along the three rotation axes. The first degree of freedom is the angular velocity of both flywheels. The second is the differential angular velocity between the two flywheels. And the remaining two degrees of freedom correspond to Vernier gimbaling along two axes, enabled by the radial active magnetic bearings of both flywheels.

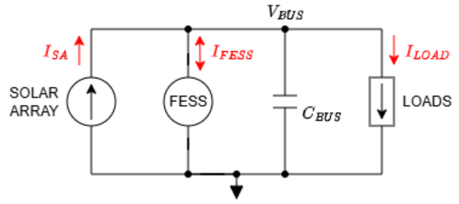

Fig. 1. Simplified schematic of a satellite electrical power system, including the solar arrays, the Flywheel Energy Storage System (FESS), the bus capacitor, and the loads.

Once integrated into a satellite platform, as illustrated in Fig. 1, the FESS will be controlled to regulate its current to maintain the voltage across the bus capacitor, similarly to a conventional regulated power bus, thereby enabling battery-like operation. Nevertheless, the inclusion of a small battery in parallel will likely remain necessary, both to support mission start-up and to define the bus impedance.

The use case currently considered for the preliminary sizing of the system is a typical telecommunications LEO satellite, representative of the upper range of the small satellite category. Although the total onboard battery capacity exceeds 15 kWh, only approximately 1.8 kWh is effectively required to meet mission needs, with a peak output power of 8 kW. Assuming a Depth of Discharge (DoD) of 75%, as commonly reported in the literature (among others in [4], [5], [7], [8] and [13]), the total required stored energy for the FESS is therefore estimated at approximately 2.5 kWh at maximum velocity.

B. Flywheel dimensions, mass and inertia

To analyze the impact of both flywheels composing the FESS on satellite attitude, a simplified model of these flywheels is developed to estimate key parameters such as maximum angular velocity, dimensions, inertia, and mass. But to estimate these key parameters, it is first necessary to consider candidate materials based on their theoretical specific energy, as defined in (1), where K denotes the shape factor [63]. For comparison, state-of-the-art space-qualified batteries exhibit specific energies on the order of 180 Wh/kg at 100% DoD [64]. As illustrated in Fig. 2, achieving comparable specific energies with flywheels requires the use of high-performance composite materials, such as carbon fiber, due to the unfavorable tensile strength-to-density ratio of metallic materials. To retain design margin for future optimization, M40J carbon fiber (~200Wh/kg) is selected as the reference material for the flywheel design.

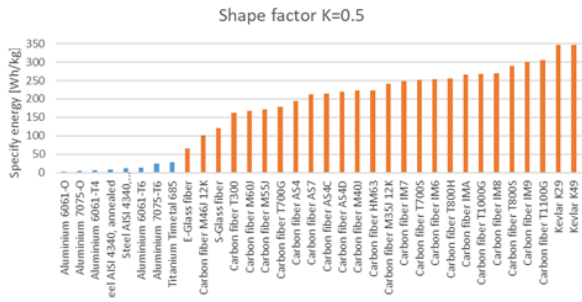

Fig. 2. Specific energy of selected metallic and composite materials, assuming an average shape factor of 0.5.

$$\frac{E}{m} = K\frac{\sigma}{\rho} \quad (1)$$

Considering Depth of Discharge and structural mass, FESS can substantially reduce onboard energy storage mass compared with batteries. For example, batteries with a DoD below 20% have an effective specific energy under 36 Wh/kg, whereas FESS with a 75% DoD, even accounting for a tripling of mass due to the structure, achieves 50 Wh/kg. This advantage increases further for lower battery DoD or for an optimized FESS structure, highlighting the potential of FESS for lighter, more efficient satellite energy storage systems.

Then, based on the previously defined energy storage requirement and the selected material, each flywheel is modeled as a simple thin cylindrical rim with a massless shaft, and its main parameters are obtained through a constrained optimization process. The first condition ensures that the total kinetic energy (2) exceeds 2.5 kWh at maximum angular velocity, where ω is the angular velocity and I is the axial moment of inertia. The second and third conditions impose that the radial and tangential stresses at maximum angular velocity remain below the material tensile strength, with appropriate safety margins. Finally, the fourth and fifth conditions aim at minimizing the flywheel mass and volume.

$$E = \frac{I\omega^2}{2} \quad (2)$$

Based on these conditions, it is then possible to optimize the four parameters defining the flywheel: the maximum angular velocity ω_{MAX}, the inner R_{IN} and outer R_{OUT} radii of the rim, and the flywheel length L. The optimized parameters are presented in TABLE I. The resulting flywheel axial inertia is 0.33 kg.m², with a mass of 8.2 kg (for each flywheel).

TABLE I. FLYWHEEL OPTIMIZED PARAMETERS.

Parameters	**Values**	**Units**
Angular velocity @ 2.5kWh	50	krpm
Inner radius	18.13	cm
Outer radius	21.89	cm
Flywheel length (each)	11.07	cm

C. FESS control

Satellite power buses can be either regulated or unregulated. In regulated architectures, the Flywheel Energy Storage System can replace the battery and its Battery Charge and Discharge Regulator (BCDR) to control the bus capacitor voltage. However, depending on the dynamic response of the FESS, a small battery or (super)capacitors may still be required in parallel. In unregulated architectures, a small battery will likely remain necessary to ensure voltage stability, while the FESS operates as a bidirectional current source.

In both cases, the FESS is driven by a power reference which, assuming constant bus voltage, is equivalent to a current reference. This reference is converted into torque commands for both flywheels, as illustrated in Fig. 3. Internal controllers regulate the motors to track these torque commands, enabling energy storage through acceleration and energy delivery through deceleration.

In parallel, a dedicated torque control loop compensates for disturbances induced by both flywheel rotations, thereby limiting their impact on satellite attitude. This is achieved through the control of the angular velocity differential between the two wheels, as well as the actuation of the active magnetic bearings using Vernier gimballing. Ideally, the FESS should operate independently of the Attitude and Orbit Control Subsystem (AOCS). However, this assumption requires further validation.

IV. FESS ATTITUDE IMPACT MODELING AND SIMULATION

A. Dynamic modeling

To analyze the dynamic behavior, the system is simplified to a rigid multibody model comprising the satellite and the rotors of both flywheels. The corresponding reference frames are defined in Fig. 4, with $\{\hat{\boldsymbol{I}}\}$ representing the inertial frame, $\{\hat{\boldsymbol{X}}^1\}$ the satellite body-frame, $\{\hat{\boldsymbol{X}}^2\}$ and $\{\hat{\boldsymbol{X}}^4\}$ the stator body-frames of the two flywheels (fixed with respect to $\{\hat{\boldsymbol{X}}^1\}$), and $\{\hat{\boldsymbol{X}}^3\}$ and $\{\hat{\boldsymbol{X}}^5\}$ the rotor body-frames of both flywheels. For the dynamic analysis, the FESS is not modeled as a single entity but through the combined contributions of both flywheels. Its effect on the satellite is represented solely by the resulting torque expressed in the satellite body-frame.

In addition, any vector $\boldsymbol{x}$ can be expressed in any body-frame using the notation defined in (3), where $[\hat{\boldsymbol{X}}^i]$ denotes

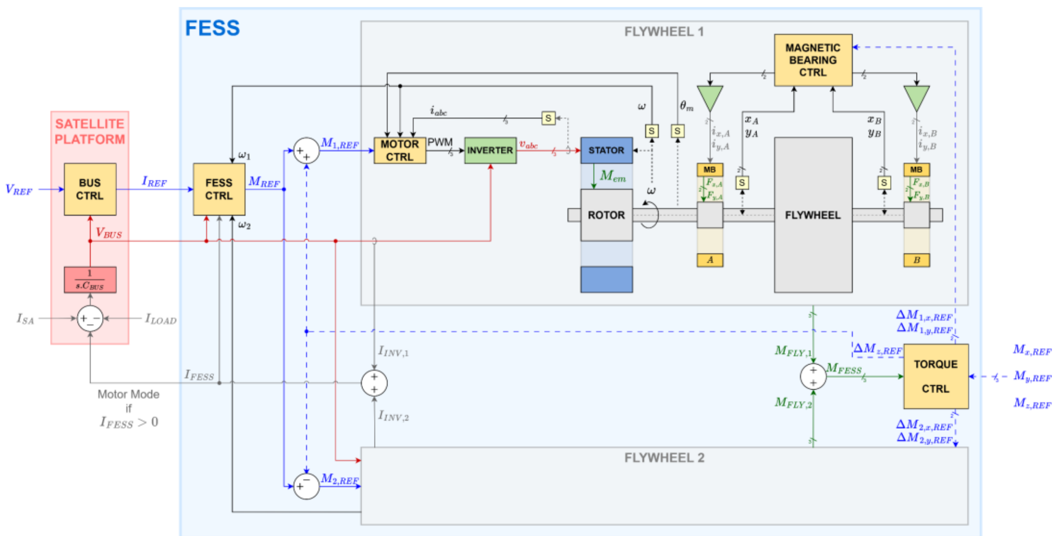

Fig. 3. Detailed block diagram of satellite power bus regulation using a Flywheel Energy Storage System composed of two magnetically suspended flywheels, including power and attitude control loops.

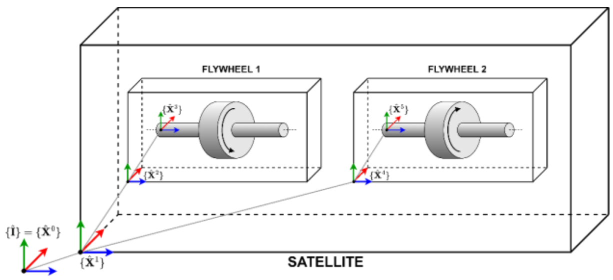

Fig. 4. Simplified representation of the satellite and both flywheels as rigid bodies (stators and rotors) with their respective body-frames, the inertial frame $\{\hat{I}\}$ being the Earth.

the column matrix of the three unit vectors of the body-frame $\{\hat{\boldsymbol{X}}^i\}$.

$$\begin{aligned} \boldsymbol{x} &= \left[\hat{\boldsymbol{X}}^i\right]^T \left[\ {}_i x_x \quad {}_i x_y \quad {}_i x_z\right]^T \\ &= {}_i x_x\, \hat{\boldsymbol{X}}^i_x + {}_i x_y\, \hat{\boldsymbol{X}}^i_y + {}_i x_z\, \hat{\boldsymbol{X}}^i_z \end{aligned} \tag{3}$$

To derive the torque interaction between the satellite and the FESS, the total angular momentum vector $\boldsymbol{H}$ is first defined in (4) as the sum of the angular momentum vectors of the three bodies, expressed w.r.t. their respective centers of mass. $\boldsymbol{I}_S$, $\boldsymbol{I}_{F_1}$ and $\boldsymbol{I}_{F_2}$ denote the inertia tensors of the satellite and of the two flywheel rotors w.r.t. their respective centers of mass, and $\boldsymbol{\omega}_S$, $\boldsymbol{\omega}_{F_1}$ and $\boldsymbol{\omega}_{F_2}$ their absolute angular velocity vectors.

$$\boldsymbol{H} = \boldsymbol{I}_S\ \boldsymbol{\omega}_S\ + \boldsymbol{I}_{F_1}\ \boldsymbol{\omega}_{F_1} + \boldsymbol{I}_{F_2} \boldsymbol{\omega}_{F_2} \tag{4}$$

The time derivative of $\boldsymbol{H}$ yields the total pure torque vector, developed in (5).

$$\begin{aligned} \dot{\boldsymbol{H}} &= \boldsymbol{I}_S\ \dot{\boldsymbol{\omega}}_S + \boldsymbol{\omega}_S \times \boldsymbol{I}_S\ \boldsymbol{\omega}_S \\ &+ \boldsymbol{I}_{F_1}\ \dot{\boldsymbol{\omega}}_{F_1} + \boldsymbol{\omega}_{F_1} \times \boldsymbol{I}_{F_1}\ \boldsymbol{\omega}_{F_1} \\ &+ \boldsymbol{I}_{F_2}\ \dot{\boldsymbol{\omega}}_{F_2} + \boldsymbol{\omega}_{F_2} \times \boldsymbol{I}_{F_2}\ \boldsymbol{\omega}_{F_2} \end{aligned} \tag{5}$$

Introducing $\boldsymbol{\Omega}_{F_i}$ the angular velocity vector of each rotor relative to the satellite body-frame, the rotor absolute angular velocity vectors can be expressed as $\boldsymbol{\omega}_{F_i} = \boldsymbol{\Omega}_{F_i} + \boldsymbol{\omega}_S$ leading to the expanded torque expression in (6).

$$\begin{aligned} \dot{\boldsymbol{H}} &= \boldsymbol{I}_S\ \dot{\boldsymbol{\omega}}_S + \boldsymbol{\omega}_S \times \boldsymbol{I}_S\ \boldsymbol{\omega}_S \\ &+ \boldsymbol{I}_{F_1} \left(\dot{\boldsymbol{\Omega}}_{F_1} + \boldsymbol{\omega}_S \times \boldsymbol{\Omega}_{F_1} + \dot{\boldsymbol{\omega}}_S\right) \\ &+ \left(\boldsymbol{\Omega}_{F_1} + \boldsymbol{\omega}_S\right) \times \boldsymbol{I}_{F_1} \left(\boldsymbol{\Omega}_{F_1} + \boldsymbol{\omega}_S\right) \\ &+ \boldsymbol{I}_{F_2} \left(\dot{\boldsymbol{\Omega}}_{F_2} + \boldsymbol{\omega}_S \times \boldsymbol{\Omega}_{F_2} + \dot{\boldsymbol{\omega}}_S\right) \\ &+ \left(\boldsymbol{\Omega}_{F_2} + \boldsymbol{\omega}_S\right) \times \boldsymbol{I}_{F_2} \left(\boldsymbol{\Omega}_{F_2} + \boldsymbol{\omega}_S\right) \end{aligned} \tag{6}$$

Assuming the absence of external torques ($\dot{\boldsymbol{H}} = \boldsymbol{0}$), the pure torque vector $\boldsymbol{M}_S$ exerted on the satellite by the FESS is expressed in (7), where the contribution of each rotor is defined in (8).

$$\begin{aligned} \boldsymbol{M}_S &= \boldsymbol{I}_S\ \dot{\boldsymbol{\omega}}_S + \boldsymbol{\omega}_S \times \boldsymbol{I}_S\ \boldsymbol{\omega}_S \\ &= -\left(\boldsymbol{M}_{F_1} + \boldsymbol{M}_{F_2}\right) \\ &= -\boldsymbol{M}_{FESS} \end{aligned} \tag{7}$$

$$\begin{aligned} \boldsymbol{M}_{F_i} &= \boldsymbol{I}_{F_i} \left(\dot{\boldsymbol{\Omega}}_{F_i} + \boldsymbol{\omega}_S \times \boldsymbol{\Omega}_{F_i} + \dot{\boldsymbol{\omega}}_S\right) \\ &+ \left(\boldsymbol{\Omega}_{F_i} + \boldsymbol{\omega}_S\right) \times \boldsymbol{I}_{F_i} \left(\boldsymbol{\Omega}_{F_i} + \boldsymbol{\omega}_S\right) \end{aligned} \tag{8}$$

Starting from the general pure torque expressions in (7) and (8), a simplified formulation can be derived for nominal operation in the absence of non-idealities. Under continuous Earth-pointing conditions, the satellite undergoes a constant pitch rotation (y-axis), such that $\boldsymbol{\omega}_S \approx \left[\hat{\boldsymbol{X}}^1\right]^T [0 \quad \omega_S \quad 0]^T$. Assuming the flywheel rotors are aligned with the satellite yaw axis (z-axis), the rotor relative angular velocity vectors reduce to $\boldsymbol{\Omega}_{F_i} \approx \left[\hat{\boldsymbol{X}}^1\right]^T [0 \quad 0 \quad \Omega_{F_i}]^T$ leading to (9).

$$\boldsymbol{\Omega}_{F_i} + \boldsymbol{\omega}_S \approx \left[\hat{\boldsymbol{X}}^1\right]^T [0 \quad \omega_S \quad \Omega_{F_i}]^T \tag{9}$$

Finally, assuming that each rotor body-frame is aligned with its principal axes of inertia and that $I_{xx} = I_{yy}$, each rotor pure torque vector simplifies to (10), revealing two torque components: the electromagnetic torque $M_{em,F_i} = I_{zz}\dot{\Omega}_{F_i}$ and the gyroscopic torque $\omega_S I_{zz} \Omega_{F_i}$. This gyroscopic torque must be compensated by the magnetic bearings to maintain rotor orientation. Otherwise, it induces a rotation of the satellite.

$$\boldsymbol{M}_{F_i} \approx \left[\hat{\boldsymbol{X}}^1\right]^T \begin{bmatrix} \omega_S I_{zz} \Omega_{F_i} \\ 0 \\ I_{zz} \dot{\Omega}_{F_i} \end{bmatrix} \approx \left[\hat{\boldsymbol{X}}^1\right]^T \begin{bmatrix} \omega_S I_{zz} \Omega_{F_i} \\ 0 \\ M_{em,F_i} \end{bmatrix} \tag{10}$$

And since the two rotors operate at opposite velocities in the satellite body-frame $\{\hat{\boldsymbol{X}}^1\}$ ($\Omega_{F_1} = -\Omega_{F_2}$), their contributions cancel, resulting in zero net torque on the satellite under nominal conditions.

B. Simulation model

The pure torque vector defined in (10) provides a convenient first-order approximation of the system dynamics but fails to capture higher-order coupling effects and modeling discrepancies. In contrast, the formulations in (7) and (8) offer a complete vectorial description of the system, at the expense of significantly increased analytical complexity, making manual derivation cumbersome.

To bridge this gap, a rigid-body model was implemented in Robotran [65], [66]. This multibody approach allows for the explicit definition of all relevant degrees of freedom, kinematic constraints, and inertial couplings, enabling accurate dynamic simulation of the system and validation of control strategies for both energy storage and torque control. The model enables efficient computation of internal forces and torques, as well as precise evaluation of the coupling between the FESS and the satellite platform, including its impact on spacecraft attitude dynamics.

C. Nominal operating scenario

The developed Robotran model enables the simulation of a representative operating scenario to assess both the impact of the satellite rotation on the flywheels and the influence of the flywheels on the satellite dynamics. In its current form, the model provides the energy stored in the FESS, and the efforts between the satellite and the FESS. To ease the primary analysis, the wheels are positioned symmetrically about the satellite's center of mass but with opposite directions. The primary input parameter is the required FESS power. The model can further be extended to include additional inputs, such as torque imbalance between the two flywheels (section V), and rotor orientations, thereby enabling three-axis torque control, as illustrated in Fig. 3.

The operating scenario is divided into five phases:

1. FESS start-up under torque saturation to limit winding and inverter currents (to avoid excessive losses), up to 75% DoD;
2. FESS charging at maximum power (8 kW) up to full charge (0% DoD);
3. FESS state of charge maintained at 0% DoD;
4. FESS discharge at maximum power (8 kW) down to 75% DoD;
5. FESS state of charge maintained at 75% DoD.

The simulated scenario is presented in Fig. 5, showing the relative angular velocities of both rotors with respect to their stators, the electromagnetic torques applied by both stators, as well as the resulting FESS power and stored energy. As expected, the stored energy reaches 2500 Wh at a rotor angular velocity of 50 krpm (5236 rad/s), as defined in Table I.

The torques $\dot{H}_x^O$, $\dot{H}_y^O$ and $\dot{H}_z^O$ with respect to the origin O of the inertial frame $\{\hat{\boldsymbol{I}}\}$ shown in Fig. 6 can be readily verified using (10), considering an orbital period of 100 minutes, which corresponds to a satellite pitch angular velocity of approximately 1 mrad/s. The estimated gyroscopic torque is 1.73 Nm, which is in close agreement with the simulated value. The maximum electromagnetic torque applied to each rotor corresponds to half of the FESS maximum power divided by the rotor angular velocity at 75% DoD. This yields 1.53 Nm, consistent with the simulation results.

Additionally, a force is observed along the z-axis, corresponding to the centripetal force induced by the satellite rotation, as the flywheels are not located at the satellite center of mass. Considering a distance of 0.5 m, the resulting force is estimated at 4.1 µN.

D. *Non-idealities analysis*

1) *Overview*

Under nominal conditions, although internal torques exist between the satellite and the two flywheel rotors, the net torque exerted by the FESS on the satellite is zero, as the contributions cancel each other. However, in practice, several non-idealities arise and must be considered, as they can generate parasitic torques if not properly controlled, thereby affecting the satellite attitude. The main non-idealities include:

1. **Alignment mismatch** between the two rotors, resulting in an orthogonal component of angular momentum;
2. **Inertia mismatch**, since the two flywheels cannot be perfectly identical even with the same manufacturing process;
3. **Electromagnetic torque mismatch** between the motors, which may arise from factors such as permanent magnet tolerances;
4. **Rotor static/dynamic imbalance**, leading to high-frequency oscillations.

2) *Alignment mismatch*

Perfect cancellation of the torque contributions requires both rotors to be aligned along the same axis. Any deviation from this configuration results in the emergence of an

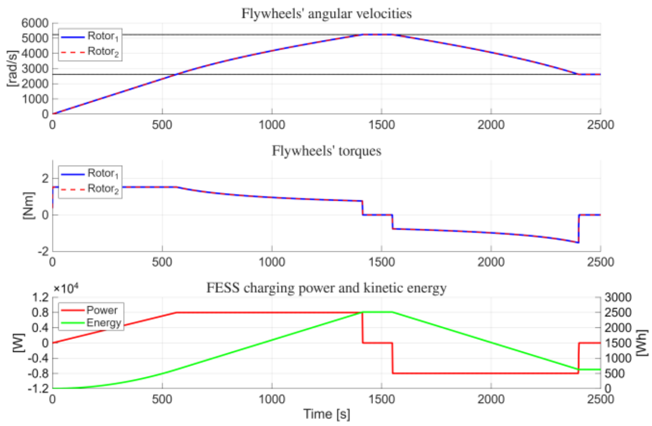

Fig. 5. Robotran simulation of the nominal charge and discharge operating scenario, preceded by the FESS start-up.

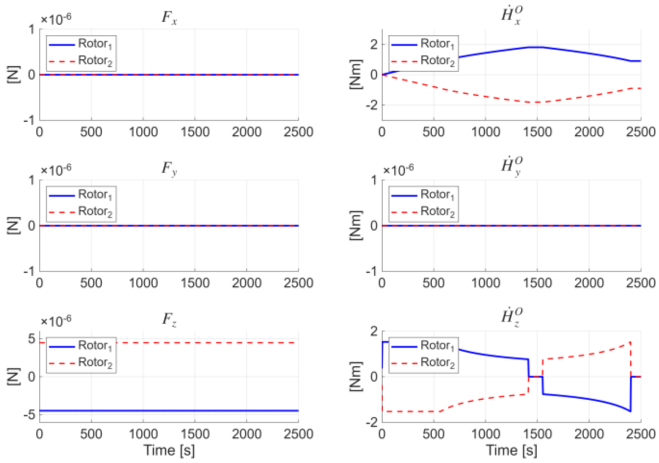

Fig. 6. Simulated forces and torques (w.r.t. the origin O of the inertial frame) between the flywheel rotors and the FESS for the nominal operating scenario.

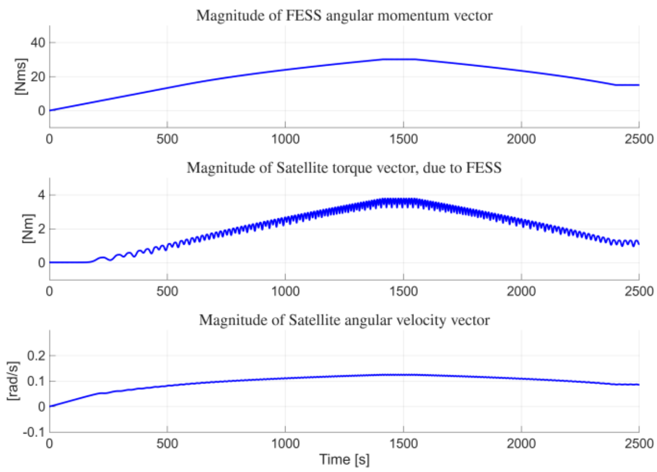

Fig. 7. Robotran simulation results illustrating the effect of a 1° misalignment of one rotor in the FESS.

orthogonal angular momentum component, giving rise to gyroscopic torques and consequently inducing rotation of the satellite. By introducing a misalignment of 1°, this orthogonal angular momentum reaches up to 30 Nms at maximum angular velocity. This parasitic angular momentum is of the same order of magnitude as that of commercial momentum wheels used in space applications and is therefore non-negligible.

The amplitude of this parasitic angular momentum in the FESS is confirmed by the Robotran simulation results shown in Fig. 7. It induces a torque on the satellite with a magnitude of approximately 4 Nm at maximum velocity, resulting in a satellite angular velocity reaching 0.12 rad/s (6.8°/s). This is significantly higher than the satellite pitch angular velocity, and therefore represents an unacceptable perturbation induced by the FESS that must be controlled.

3) Inertia mismatch

Although current manufacturing techniques allow for very high repeatability, the two flywheel rotors can never be perfectly identical. As a result, their respective inertia matrices will differ. In the case of an axial inertia mismatch, the impact remains limited: it affects only the stored energy and does not influence the satellite attitude, provided that this is the sole non-ideality. Indeed, since both stators apply identical torques (as illustrated in Fig. 3), the net torque exerted by the FESS on the satellite is zero. Consequently, while the flywheels may reach different angular velocities, their angular momenta remain equal in magnitude and opposite in direction, as they result from the time integration of identical electromagnetic torques. Regarding a radial inertia mismatch, it has no impact if it is the only non-ideality, as it does not appear in (10).

4) Electromagnetic torque mismatch

Several factors may lead to an electromagnetic torque mismatch between the two motors. In practice, the control regulates the stator currents rather than the torque directly. One source of mismatch stems from manufacturing tolerances in the permanent magnets, whose magnetic properties are typically specified with variations ranging from 10% to 25%. Another source is the inaccuracy in stator current measurements, which can typically reach 1%.

This non-ideality directly affects the energy storage function of the FESS, as well as the actual power delivered compared to the target value. However, it can be compensated at the system level by the FESS control scheme shown in Fig. 3, which adjusts the required power based on a measurement of the FESS input current. Nevertheless, this approach does not correct the dynamical impact on the satellite, which can only be mitigated through a dedicated torque control loop based on torque feedback. A single-axis torque control strategy is sufficient to compensate for this mismatch by acting on the parameter $\Delta M_{z,REF}$ shown in Fig. 3, as demonstrated in section V.

For a simulated torque mismatch of 10% in the Robotran model (illustrated in Fig. 8), the impact on the satellite attitude is severe, with the angular velocity magnitude reaching approximately 3.25 rad/s (186°/s). This results from the FESS angular momentum, which reaches 325 Nms, thereby generating gyroscopic torques that add to the axial torque mismatch, leading to a total FESS torque magnitude of approximately 0.33 Nm.

5) Rotor imbalance

A static or dynamic imbalance in a rotor originates from the presence of a small parasitic mass on the wheel. Although negligible with respect to the total rotor mass, this perturbation induces a shift in the center of mass and modifies the principal axes of inertia. As a result, the Flywheel Energy Storage System (FESS) exhibits high-frequency oscillations. These oscillations affect the satellite attitude. While no net rotation

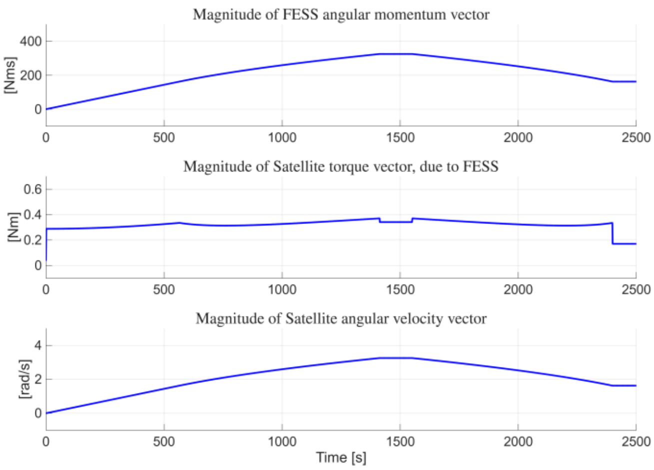

Fig. 8. Robotran simulation results showing the impact of a 10% electromagnetic torque mismatch between the two flywheel motors.

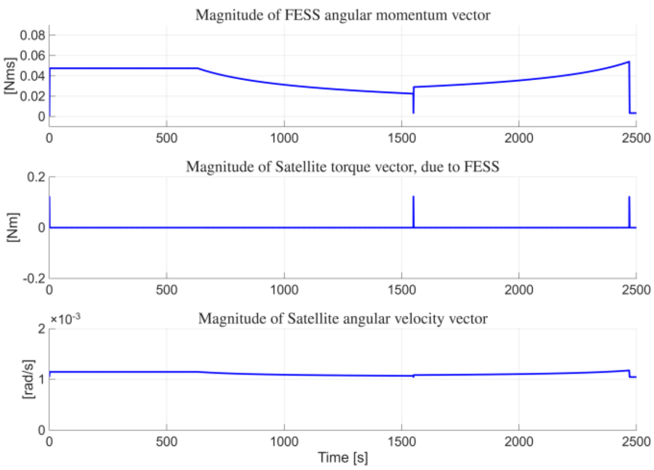

Fig. 9. Robotran simulation results demonstrating the effectiveness of z-axis torque control in compensating for a 10% electromagnetic torque mismatch between the two flywheel motors.

of the satellite is induced, the resulting oscillatory motion can degrade mission performance, particularly for payloads requiring high pointing stability. In addition, the imbalance may lead to increased power consumption due to the control effort required to attenuate these oscillations [11], [52], notably through the active magnetic bearings. If the torque control bandwidth is not sufficiently high to effectively reject these oscillations, a dedicated control strategy may be required to mitigate their impact.

V. Torque Control

The axial FESS torque, induced by a mismatch between the electromagnetic torques of the two motors, can be effectively compensated by the torque controller (Fig. 3) using the measured axial pure torque M_z between the FESS and the satellite. The corresponding correction $\Delta M_{z,REF}$, defined in (11), is generated by a proportional–integral controller with gains $K_{z,P}$ and $K_{z,I}$, and is directly applied to the motor torque references $M_{1,REF}$ and $M_{2,REF}$, as defined in (12). Here, M_{REF} denotes the pure torque reference provided by the FESS controller, which regulates the system power, and so the FESS current.

$$\Delta M_{z,REF} = \frac{K_{z,P} \cdot s + K_{z,I}}{s} \left(M_{z,REF} - M_z \right) \qquad (11)$$

$$
\begin{aligned}
M_{1,REF} &= M_{REF} + \frac{\Delta M_{z,REF}}{2} \\
M_{2,REF} &= M_{REF} - \frac{\Delta M_{z,REF}}{2}
\end{aligned} \tag{12}
$$

The Robotran simulation presented in Fig. 9 demonstrates that the controller effectively compensates for the 10% mismatch between the motor torques, thereby significantly reducing its impact on the satellite attitude. However, as the compensation is not instantaneous, the AOCS would still be required to reject residual perturbations, although they remain negligible. These residual effects arise from the small angular momentum of the FESS, which, in the presence of gyroscopic coupling, generates torques on the order of a few micro–Newton meters. The resulting parasitic angular velocity magnitude is below 1 mrad/s (0.057°/s).

VI. Conclusion

While a comprehensive review of the state of the art confirms that the use of flywheels for onboard energy storage in satellites is not a novel concept, both technological capabilities and mission requirements have significantly evolved. Moreover, Flywheel Energy Storage Systems remain highly competitive with chemical batteries in terms of mass and volume, primarily due to their high Depth of Discharge capability. This can lead to reduced launch mass and more compact satellite designs.

In this context, this work introduces a standalone, battery-like Flywheel Energy Storage System based on two magnetically suspended counter-rotating flywheels. The considered system is designed to store up to 2.5 kWh at maximum angular velocity, with peak charge and discharge power of 8 kW, thereby constituting a credible energy storage alternative to conventional batteries.

In the presence of non-idealities, non-negligible parasitic torques arise between the FESS and the satellite, leading to attitude disturbances that must be compensated by the Attitude and Orbit Control System. Fortunately, the preliminary analysis demonstrates that the introduction of a dedicated torque controller enables effective cancellation of these parasitic torques. While axial torque control has been successfully tested in this work, subsequent efforts will focus on implementing a full three-axis torque control strategy, leveraging magnetic bearings to suppress all disturbance torques transmitted from the FESS to the satellite. In addition, the entire power chain between the satellite power bus and the flywheel system, including the inverters and electric machines, will be investigated to validate the feasibility of the concept for space applications.

References

[1] J. E. Notti, A. Cormack, and W. C. Schmill, "Integrated Power/Attitude Control System (IPACS) study. Volume 1: Feasibility studies," Rockwell International, NASA CR-2383, Apr. 1974. Accessed: Jul. 16, 2025. [Online]. Available: https://ntrs.nasa.gov/citations/19740014593

[2] J. E. Notti, A. Cormack, and W. J. Klein, "Integrated Power/Attitude Control System (IPACS)," Journal of Spacecraft and Rockets, vol. 12, no. 8, pp. 485–491, Aug. 1975, doi: 10.2514/3.57006.

[3] C. R. Keckler, "Integrated Power/Attitude Control System (IPACS)," presented at the Integrated Flywheel Technology, Dec. 1983. [Online]. Available: https://ntrs.nasa.gov/citations/19840004161

[4] G. E. Rodriguez, P. A. Studer, and D. A. Baer, "Assessment of flywheel energy storage for spacecraft power systems," Goddard Space Flight Center, Technical Memorandum NASA-TM-85061, Jan. 1983. Accessed: Jul. 18, 2025. [Online]. Available: https://ntrs.nasa.gov/citations/19830025670

[5] G. E. Rodriguez, "Inertial Energy Storage for Spacecraft," The 1983 Goddard Space Flight Center Battery Workshop, Jan. 1984, Accessed: Jul. 18, 2025. [Online]. Available: https://ntrs.nasa.gov/citations/19840025598

[6] G. E. Santo, S. P. Gill, J. F. Kotas, and R. Paschall, "Feasibility of flywheel energy storage systems for applications in future space missions," Rockwell International, NASA-CR-195422, Jan. 1995. Accessed: Jul. 18, 2025. [Online]. Available: https://ntrs.nasa.gov/citations/19950019973

[7] T. J. Pieronek, D. K. Decker, and V. A. Spector, "Spacecraft flywheel systems-benefits, and issues," in Proceedings of the IEEE 1997 National Aerospace and Electronics Conference. NAECON 1997, Jul. 1997, pp. 589–593 vol.2. doi: 10.1109/NAECON.1997.622703.

[8] D. A. Christopher and R. Beach, "Flywheel technology development program for aerospace applications," IEEE Aerospace and Electronic Systems Magazine, vol. 13, no. 6, pp. 9–14, Jun. 1998, doi: 10.1109/62.683723.

[9] J. B. Roes, "An electro-mechanical energy storage system for space application," in Energy Conversion for Space Power, Elsevier, 1961, pp. 613–622. doi: 10.1016/B978-0-12-395560-9.50043-4.

[10] R. Sindlinger, "Magnetic Bearing Momentum Wheels with Vernier Gimballing Capability for 3-Axis Active Attitude Control and Energy Storage," IFAC Proceedings Volumes, vol. 9, no. 1, pp. 849–860, May 1976, doi: 10.1016/S1474-6670(17)67168-4.

[11] P. C. Poubeau, "Satellite Flywheels with Magnetic Bearings and Passive Radial Centering," Journal of Spacecraft and Rockets, vol. 17, no. 2, pp. 93–98, Mar. 1980, doi: 10.2514/3.57713.

[12] A. A. Robinson, "European development experience on energy storage wheels for space," NASA. Langley Research Center An Assessment of Integrated Flywheel System Technol., Jan. 1984, Accessed: Jan. 07, 2026. [Online]. Available: https://ntrs.nasa.gov/citations/19850005547

[13] R. E. Oglevie and D. B. Eisenhaure, "Advanced Integrated Power and Attitude Control System (IPACS) study," Contractor Report 3912, Jan. 1985. Accessed: Jul. 18, 2025. [Online]. Available: https://ntrs.nasa.gov/citations/19860005868

[14] J. Edwards, J. W. Aldrich, D. A. Christopher, R. F. Beach, and J. R. Barton, "Flight test demonstration of a flywheel energy storage system on the International Space Station," in Proceedings of the IEEE 1997 National Aerospace and Electronics Conference. NAECON 1997, Jul. 1997, pp. 617–621 vol.2. doi: 10.1109/NAECON.1997.622707.

[15] B. G. Beaman and G. M. Rao, "Hybrid battery and flywheel energy storage system for LEO spacecraft," in Thirteenth Annual Battery Conference on Applications and Advances. Proceedings of the Conference, Jan. 1998, pp. 113–116. doi: 10.1109/BCAA.1998.653851.

[16] N. Groom and C. Britcher, "Fifth International Symposium on Magnetic Suspension Technology," Langley Research Center, Conference Proceedings 20000089691, Jul. 2000. [Online]. Available: https://ntrs.nasa.gov/citations/20000089691

[17] C. D. Hall, "High speed flywheels for integrated energy storage and attitude control," in Proceedings of the 1997 American Control Conference (Cat. No.97CH36041), Jun. 1997, pp. 1894–1898 vol.3. doi: 10.1109/ACC.1997.610914.

[18] C. M. Roithmayr, International Space Station Attitude Control and Energy Storage Experiment: Effects of Flywheel Torque, Jan. 02, 1999. Accessed: Jul. 11, 2025. [Online]. Available: https://ntrs.nasa.gov/citations/19990025459

[19] C. M. Roithmayr, "International Space Station attitude motion associated with flywheel energy storage," in AIP Conference Proceedings, Seoul (Korea): AIP, 2000, pp. 454–459. doi: 10.1063/1.1302521.

[20] C. M. Roithmayr, "Dynamics and Control of Attitude, Power, and Momentum for a Spacecraft Using Flywheels and Control Moment Gyroscopes," NASA, Langley Research Center, Hampton, Virginia, TP–2003–212178, 2003. [Online]. Available: https://www.cs.odu.edu/~mln/ltrs-pdfs/NASA-2003-tp212178.pdf

[21] C. M. Roithmayr, C. D. Karlgaard, R. R. Kumar, and D. M. Bose, "Integrated Power and Attitude Control with Spacecraft Flywheels and Control Moment Gyroscopes," Journal of Guidance, Control, and Dynamics, vol. 27, no. 5, pp. 859–873, Sep. 2004, doi: 10.2514/1.2096.

[22] P. E. Kascak, B. H. Kenny, T. P. Dever, W. Santiago, and R. H. Jansen, "International Space Station Bus Regulation With NASA Glenn Research Center Flywheel Energy Storage System Development Unit," presented at the 36th Intersociety Energy Conversion Engineering

Conference, Jan. 2001. Accessed: Jul. 11, 2025. [Online]. Available: https://ntrs.nasa.gov/citations/20020018026

[23] B. H. Kenny, P. E. Kascak, H. Hofmann, M. Mackin, W. Santiago, and R. Jansen, "Advanced Motor Control Test Facility for NASA GRC Flywheel Energy Storage System Technology Development Unit," presented at the 36th Intersociety Energy Conversion Engineering Conference, Jan. 2001. Accessed: Jul. 11, 2025. [Online]. Available: https://ntrs.nasa.gov/citations/20010090467

[24] B. H. Kenny and P. E. Kascak, "Sensorless Control of Permanent Magnet Machine for NASA Flywheel Technology Development," presented at the 37th Intersociety Energy Conversion Engineering Conference, Jan. 2002. Accessed: Jul. 11, 2025. [Online]. Available: https://ntrs.nasa.gov/citations/20020070607

[25] B. H. Kenny, P. E. Kascak, R. Jansen, and T. Dever, "A flywheel energy storage system demonstration for space applications," in *IEEE International Electric Machines and Drives Conference, 2003. IEMDC'03.*, Jun. 2003, pp. 1314–1320 vol.2. doi: 10.1109/IEMDC.2003.1210409.

[26] B. H. Kenny and P. E. Kascak, "DC Bus Regulation with a Flywheel Energy Storage System," presented at the Power Systems Conference, Jan. 2003. Accessed: Jul. 17, 2025. [Online]. Available: https://ntrs.nasa.gov/citations/20030016686

[27] P. Kascak, R. Jansen, B. Kenny, and T. Dever, "Demonstration of attitude control and bus regulation with flywheels," in *Conference Record of the 2004 IEEE Industry Applications Conference, 2004. 39th IAS Annual Meeting.*, Oct. 2004, pp. 2018–2029 vol.3. doi: 10.1109/IAS.2004.1348745.

[28] B. H. Kenny, R. Jansen, P. Kascak, T. Dever, and W. Santiago, "Demonstration of single axis combined attitude control and energy storage using two flywheels," in *2004 IEEE Aerospace Conference Proceedings (IEEE Cat. No.04TH8720)*, Mar. 2004, pp. 2801-2819 Vol.4. doi: 10.1109/AERO.2004.1368077.

[29] B. H. Kenny, R. Jansen, P. Kascak, T. Dever, and W. Santiago, "Integrated power and attitude control with two flywheels," *IEEE Transactions on Aerospace and Electronic Systems*, vol. 41, no. 4, pp. 1431–1449, Oct. 2005, doi: 10.1109/TAES.2005.1561894.

[30] B. H. Kenny, P. E. Kascak, R. Jansen, T. Dever, and W. Santiago, "Control of a high-speed flywheel system for energy storage in space applications," *IEEE Transactions on Industry Applications*, vol. 41, no. 4, pp. 1029–1038, Jul. 2005, doi: 10.1109/TIA.2005.851021.

[31] R. Jansen and T. Dever, "G2 Flywheel Module Design," in *2nd International Energy Conversion Engineering Conference*, Providence, Rhode Island: American Institute of Aeronautics and Astronautics, Aug. 2004. doi: 10.2514/6.2004-5603.

[32] L. V. Truong, F. J. Wolff, and N. V. Dravid, "Simulation of flywheel electrical system for aerospace applications," in Collection of Technical Papers. 35th Intersociety Energy Conversion Engineering Conference and Exhibit (IECEC) (Cat. No.00CH37022), Jul. 2000, pp. 601–608 vol.1. doi: 10.1109/IECEC.2000.870824.

[33] J. L. Fausz and D. J. Richie, "Flywheel simultaneous attitude control and energy storage using a VSCMG configuration," in Proceedings of the 2000. IEEE International Conference on Control Applications. Conference Proceedings (Cat. No.00CH37162), Sep. 2000, pp. 991–995. doi: 10.1109/CCA.2000.897602.

[34] D. J. Richie, P. Tsiotras, and J. L. Fausz, "Simultaneous attitude control and energy storage using VSCMGs: theory and simulation," in Proceedings of the 2001 American Control Conference. (Cat. No.01CH37148), Arlington, VA, USA: IEEE, 2001, pp. 3973–3979 vol.5. doi: 10.1109/ACC.2001.946291.

[35] D. J. Richie, P. Tsiotras, and J. L. Fausz, "Variable Speed Control Moment Gyroscope Workbench: a new simulation tool for tomorrow's spacecraft," in 20th DASC. 20th Digital Avionics Systems Conference (Cat. No.01CH37219), Oct. 2001, p. 8A3/1-8A3/12 vol.2. doi: 10.1109/DASC.2001.964219.

[36] P. Tsiotras, H. Shen, and C. Hall, "Satellite Attitude Control and Power Tracking with Energy/Momentum Wheels," *Journal of Guidance, Control, and Dynamics*, vol. 24, no. 1, pp. 23–34, Jan. 2001, doi: 10.2514/2.4705.

[37] P. Guyot, H. Barde, and G. Griseri, "Flywheel Power and Attitude Control Systems (FPACS)," Spacecraft Guidance, Navigation and Control Systems, vol. 425, p. 371, Feb. 2000.

[38] H. Yoon and P. Tsiotras, "Spacecraft Adaptive Attitude and Power Tracking with Variable Speed Control Moment Gyroscopes," *Journal of Guidance, Control, and Dynamics*, vol. 25, no. 6, pp. 1081–1090, Nov. 2002, doi: 10.2514/2.4987.

[39] H. Yoon, "Spacecraft Attitude and Power Control Using Variable Speed Control Moment Gyros," Georgia Institute of Technology, 2004. [Online]. Available: http://hdl.handle.net/1853/4850

[40] B. T. Costic, M. S. De Queiroz, D. M. Dawson, and Y. Fang, "Energy management and attitude control strategies using flywheels," in *Proceedings of the 40th IEEE Conference on Decision and Control (Cat. No.01CH37228)*, Orlando, FL, USA: IEEE, 2001, pp. 3435–3440. doi: 10.1109/CDC.2001.980389.

[41] Y. Jia, S. Xu, and L. Tang, "Bias Momentum Attitude Control System Using Energy/Momentum Wheels," *Chinese Journal of Aeronautics*, vol. 17, no. 4, pp. 193–199, Nov. 2004, doi: 10.1016/S1000-9361(11)60236-7.

[42] Y. Jia and S. Xu, "Spacecraft Attitude Tracking and Energy Storage Using Flywheels," *Chinese Journal of Aeronautics*, vol. 18, no. 1, pp. 1–7, Feb. 2005, doi: 10.1016/S1000-9361(11)60274-4.

[43] R. Varatharajoo and S. Fasoulas, "Methodology for the development of combined energy and attitude control systems for satellites," Aerospace Science and Technology, vol. 6, no. 4, pp. 303–311, Jun. 2002, doi: 10.1016/S1270-9638(02)01157-4.

[44] R. Varatharajoo, "A combined energy and attitude control system for small satellites," *Acta Astronautica*, vol. 54, no. 10, pp. 701–712, May 2004, doi: 10.1016/j.actaastro.2003.12.004.

[45] R. Varatharajoo and S. Fasoulas, "The combined energy and attitude control system for small satellites—Earth observation missions," Acta Astronautica, vol. 56, no. 1, pp. 251–259, Jan. 2005, doi: 10.1016/j.actaastro.2004.09.027.

[46] R. Varatharajoo, "Operation for the combined energy and attitude control system," *Aircraft Eng & Aerospace Tech*, vol. 78, no. 6, pp. 495–501, Nov. 2006, doi: 10.1108/00022660610707166.

[47] S. Eshghi and R. Varatharajoo, "Sliding Mode Control Techniques for Combined Energy and Attitude Control System," AMM, vol. 629, pp. 310–317, Oct. 2014, doi: 10.4028/www.scientific.net/AMM.629.310.

[48] S. Eshghi and R. Varatharajoo, "Nonsingular terminal sliding mode control technique for attitude tracking problem of a small satellite with combined energy and attitude control system (CEACS)," Aerospace Science and Technology, vol. 76, pp. 14–26, May 2018, doi: 10.1016/j.ast.2018.02.006.

[49] S. Aslam, Y.-C. Chak, M. H. Jaffery, and R. Varatharajoo, "The fuzzy PD control for combined energy and attitude control system," AEAT, vol. 94, no. 10, pp. 1806–1824, Dec. 2022, doi: 10.1108/AEAT-05-2021-0144.

[50] J. Park, A. Palazzolo, and R. Beach, "IPAC of a Satellite Via Magnetic Bearing Supported, Flexible Shaft Flywheels," in AIAA Guidance, Navigation, and Control Conference and Exhibit, Keystone, Colorado: American Institute of Aeronautics and Astronautics, Aug. 2006. doi: 10.2514/6.2006-6803.

[51] J. Park, A. Palazzolo, and R. Beach, "MIMO Active Vibration Control of Magnetically Suspended Flywheels for Satellite IPAC Service," Journal of Dynamic Systems, Measurement, and Control, vol. 130, no. 4, p. 041005, Jul. 2008, doi: 10.1115/1.2936846.

[52] J. Park and A. Palazzolo, "Magnetically Suspended VSCMGs for Simultaneous Attitude Control and Power Transfer IPAC Service," Journal of Dynamic Systems, Measurement, and Control, vol. 132, no. 5, p. 051001, Sep. 2010, doi: 10.1115/1.4002105.

[53] D. J. Richie, V. J. Lappas, and P. L. Palmer, "Sizing/Optimization of a Small Satellite Energy Storage and Attitude Control System," Journal of Spacecraft and Rockets, vol. 44, no. 4, pp. 940–952, Jul. 2007, doi: 10.2514/1.25134.

[54] D. J. Richie, "Combined attitude control and energy storage for small satellites using variable speed control moment," University of Surrey, Surrey (United Kingdom), 2008. [Online]. Available: https://openresearch.surrey.ac.uk/esploro/outputs/doctoral/Combined-attitude-control-and-energy-storage/99515843002346

[55] D. J. Richie, V. J. Lappas, and B. Wie, "A Practical Variable-Speed Control Moment Gyroscope Steering Law for Small Satellite Energy Storage and Attitude Control," in AIAA/AAS Astrodynamics Specialist Conference and Exhibit, Honolulu, Hawaii: American Institute of Aeronautics and Astronautics, Aug. 2008. doi: 10.2514/6.2008-7501.

[56] D. J. Richie, V. J. Lappas, and B. Wie, "Practical Steering Law for Small Satellite Energy Storage and Attitude Control," Journal of Guidance, Control, and Dynamics, vol. 32, no. 6, pp. 1898–1911, Nov. 2009, doi: 10.2514/1.41968.

[57] M. S. I. Malik and S. Asghar, "Inverse free steering law for small satellite attitude control and power tracking with VSCMGs," *Advances in Space Research*, vol. 53, no. 1, pp. 97–109, Jan. 2014, doi: 10.1016/j.asr.2013.10.001.

[58] Y. Yao, F. Liu, and H. Zhao, "Constrained steering law for VSCMGs with the function of attitude control and energy storage," Aerospace Science and Technology, vol. 58, pp. 341–350, Nov. 2016, doi: 10.1016/j.ast.2016.08.030.

[59] K. Aydin and M. T. AydemiR, "Sizing design and implementation of a flywheel energy storage system for space applications," *Turk J Elec Eng & Comp Sci*, vol. 24, pp. 793–806, 2016, doi: 10.3906/elk-1306-206.

[60] R. ÇeliKel, M. ÖzdemiR, and Ö. Aydoğmuş, "Implementation of a flywheel energy storage system for space applications," *Turk J Elec Eng & Comp Sci*, vol. 25, pp. 1197–1210, 2017, doi: 10.3906/elk-1507-259.

[61] A. I. Saad, N. H. Saad, and M. Ezzat, "Combined Power and Attitude Control System for Low Earth Orbit Satellites," in *2019 21st International Middle East Power Systems Conference (MEPCON)*, Dec. 2019, pp. 447–452. doi: 10.1109/MEPCON47431.2019.9008176.

[62] K. Sharma and A. Santasalo-Aarnio, "Energy storage systems for space applications," *Journal of Energy Storage*, vol. 128, p. 117131, Aug. 2025, doi: 10.1016/j.est.2025.117131.

[63] G. Genta, Kinetic Energy Storage: Theory and Practice of Advanced Flywheel Systems. Butterworth-Heinemann, 1985. [Online]. Available: https://doi.org/10.1016/C2013-0-00901-2

[64] Airbus Defense & Space, "ASTRO-BATT A battery product line made for LEO Radar and Optical missions," ASTRO-BATT, [Online]. Available: https://mediaassets.airbus.com/pm_38_687_687756-v579c36uso.pdf [Accessed: Mar 31, 2026].

[65] J. C. Samin and P. Fisette, "Symbolic Modelling of Multibody Systems," Kluwer Academic Publishers, 2003.

[66] N. Docquier, A. Poncelet and P. Fisette, "ROBOTRAN: a powerful symbolic generator of multibody models," Mechanical Sciences, 2013, 4, 199-219.